Hindawi
Shock and Vibration
Volume 2018, Article ID 6795763, 12 pages
https://doi.org/10.1155/2018/6795763

Research Article

Effects of Interaction between Dual Shaking Tables and Specimen and Force Feedback Compensation Control

Fangfang Li,[1] **Xiaojun Li**,[1,2] **and Juke Wang**[1]

[1]*Beijing Key Lab of Earthquake Engineering and Structural Retrofit, Beijing University of Technology, Beijing 100124, China*
[2]*Institute of Geophysics, China Earthquake Administration, Beijing 100081, China*

Correspondence should be addressed to Xiaojun Li; beerli@vip.sina.com

Received 17 May 2018; Revised 18 July 2018; Accepted 31 July 2018; Published 16 September 2018

Academic Editor: Hamid Toopchi-Nezhad

The shaking table array system is composed of multiple shaking tables for seismic response simulation tests of large-span spatial structures, bridge structures, slender structures such as pipeline and aqueduct, complex structures, and so on. In the process of testing with the multiple shaking tables, the interaction between the shaking tables and specimen affects the output accuracy of the shaking tables. The characteristics and rules of the dual shaking tables-specimen interaction effects on the system performance were analyzed in this paper. In order to improve the output accuracy of the dual shaking tables, force feedback compensation was introduced into three-variable control to reduce the interaction effects. However, the measurement errors of the force in the actuator and the acceleration of the shaking tables existed in the process of force feedback compensation. In order to verify the effectiveness of force feedback compensation for interaction between the dual shaking tables and specimen, the error influences on the system performance were simulated.

1. Introduction

An electrohydraulic shaking table can be used to simulate the real-time process of different ground motions for seismic tests of engineering structures in the laboratory. Compared with the pseudostatic test and pseudodynamic test, the shaking table test can better reflect structural responses under earthquake excitation; therefore, the shaking table is very important in earthquake engineering research field [1–5]. When analyzing the electrohydraulic shaking table system, the specimen is generally assumed to be a rigid mass in the three continuous equations of the hydraulic system [4–6]. However, because the specimen is an elastomer with large mass, the interaction between the shaking table and specimen affects the frequency response characteristic and accuracy of reproduction of the command signal. In 1988, Blondet and Esparza [7] built the analytical model including the structural specimen represented by a single DOF viscoelastic oscillator and studied the shaking table-specimen interaction effects on the shaking table system based on displacement control. The results showed that the interaction effects can lead to degradation of the performance of the shaking table, and the interaction effects are characterized by a peak-notch distortion in the amplitude-frequency response and a violent phase lag in a frequency band close to the natural frequency of the specimen. Li and Tian [8] did the theory analysis of the shaking table loaded with the N degrees of freedom specimen. It indicated that the nonlinear property of the specimen decreases the reproductive accuracy, and increasing the mass ration between the table and the specimen is one way to improve the reproductive accuracy of the shaking table. Only when the specimen mass is far less than the table mass can the nonlinear specimen effects on the performance of the system be neglected. Dyke et al. [9] discussed the importance of considering control-structure interaction when modelling a control system and developed a model including control-structure interaction (CSI) in the field of structural control for mitigation of response due to environment loads. Maoult et al. [10] did the numerical analyses on the boundary conditions between the test structure and the platform of a shaking table and verified the influence of interaction between the shaking table and specimen. Conte and Trombetti [11–13] developed a mathematic model including the shaking table base-table interaction and the table-payload interaction

and compared the numerical analysis with experimental results. The results showed that the interaction between the table and payload has more significant influence on the dynamic performance of the shaking table than the interaction between the shaking table base and table. The natural frequency of the payload becomes the second resonance frequency of the shaking table system except the oil column resonant frequency. The interaction between the shaking table and payload leads to the degradation of the performance of the shaking table. At the same time, the oil column resonant frequency decreases with the increase of the specimen mass. Li et al. [14] analyzed the influences of the specimen on stability of the shaking table system caused by SDOF and MDOF specimen models. The results showed that the stability of the shaking table designed for a nonrigid payload is greatly improved in the unload condition. Tang et al. [15] analyzed the effects of the mass, frequency, and damping ratio of the specimens on the control performance. The results showed that the mass, frequency, and damping ratio of the specimens make different degrees of influence on the interaction between the shaking table and specimen. The frequency effect is biggest of all, the damping ratio effect is secondary, and the mass effect is least. The reproduction accuracy of the command signal is poor when the frequency is close to the natural frequency of the specimen. In conclusion, the interaction effects of the shaking table and specimen on the electrohydraulic servo-shaking table system are characterized by a peak-notch distortion in the amplitude-frequency response in a frequency band close to the natural frequency of the specimen. The output of the table is affected by the shaking table-specimen interaction.

In order to improve the reproduction precision of the command signal of the shaking table, researchers did in-depth studies and developed many methods to compensate the interaction between the shaking table and specimen. Dozono et al. [16] developed adaptive filter compensation (AFC) to compensate the disturbance of the reaction force generated by a nonlinear specimen. Iwasaki et al. [17] adopted a disturbance observer-based control approach to compensate the reaction force generated by a nonlinear specimen on the shaking table. Seki et al. [18, 19] proposed an adaptive feedback compensator by applying an adaptive notch filter to identify the frequency in online manner to suppress the disturbance caused by the specimen loaded on the shaking table. Tang et al. [15] proposed a real-time compensation of reaction algorithm to improve the disadvantage caused by the interaction between the specimen and the shaking table. In the algorithm, the interaction between the shaking table and specimen was approximately calculated by the theoretical model of the specimen. The proposed control algorithm can be applied to completely compensate the disadvantage caused by the single degree of freedom specimen. However, the compensation reaction of the shaking table loaded with the multidegree of freedom specimen needs to be obtained by inertial force of the principal mode of the MDOF specimen. Phillips et al. [20] proposed a model-based multimetric control strategy applied to a small electric shaking table to improve tracking of the desired signal. In the approach, tracking over a broad frequency range was improved by using both displacement and acceleration measurements incorporated into the feedback control, the voltage command was modified through an outer-loop controller, the tracking error was reduced by applying LQR control to bring the deviation states to zero, and the transfer function iteration (TFI) was combined with the model-based feedback controller. However, velocity feedback was not included in the multimetric control strategy. Tian and Chen [21] proposed a control strategy in the shaking table test based on the elastic load. In the control strategy, the inner-loop control parameters were designed by analyzing physical models of the elastic load to realize that the transfer function of the shaking table keeps nearly unvaried with different loads. The outer-loop control was based on an adaptive control to compensate the peak and the notch generated by the elastic load. However, the apparent mass to set the parameters of the inner-loop was still obtained by the modal analysis of the elastic load.

Although the researchers already did a lot of research on the interaction between the shaking table and specimen and put forward a series of compensation control algorithms, various algorithms were for different research objects, and the scopes of application were also different. In particular, most of research studies concentrated on the interaction of a single shaking table loaded with specimen. The shaking table array system, which is composed of multiple shaking tables, can be applied for seismic response simulation tests of large-span spatial structures, bridge structures, slender structures such as pipeline and aqueduct, complex structures, and so on. The interaction forces between the multiple shaking tables and specimen are more complex than the interaction between the single shaking table and specimen, but the research on the interaction between the multiple shaking tables and specimen is lacking. The interaction effects on the system performance of the multiple shaking tables with specimen are more complicated than those of the single shaking table with specimen. Recently, the authors of this article, Li et al. [22], proposed a novel synchronous tracking strategy, differential movement synchronous tracking control (DMSTC) strategy, for double-shaking table system taking the interaction between the shaking tables and specimen into consideration. The DMSTC strategy could extend and improve the frequency bandwidth of the double-shaking table system and also improved the replication accuracy and tracking accuracy of each shaking table. In this paper, the further analysis of the interaction effects on system performance of the dual shaking tables with specimen was carried out, and force feedback compensation was introduced into three-variable control to reduce the interaction effects between the dual shaking tables and specimen. The influences of measurement errors of the force of the actuator and the acceleration of the shaking table on the system performance were simulated to verify the effectiveness of force feedback compensation.

2. Performance Analysis of Dual Shaking Tables with Specimen

In the traditional modelling of the electrohydraulic shaking table system, the table and specimen are generally assumed to be a single DOF system, and the specimen is assumed to

be a rigid mass. Equations (1)–(3) are the basic equations of the hydraulic system [4, 6], in which (1) is the equilibrium equation between the inertial force of the table and the force in the actuator.

$$M_T s^2 x = A_p p_L = F_L, \tag{1}$$

$$Q_L = A_p s x + \frac{V}{4\beta} s p_L + C_c p_L, \tag{2}$$

$$Q_L = k_q x_v - K_c p_L, \tag{3}$$

where M_T is the mass of the table, x is the piston position, A_p is the cross-sectional area of the actuator piston, p_L is the pressure difference between actuator chambers, Q_L is the total oil flow, V is the compressed oil volume in the actuator cylinder, β is the oil bulk modulus, C_c is the leakage coefficient, k_q is the flow gain, K_c is the flow-pressure coefficient, s is the Laplace transform variable, x_v is the valve spool displacement, and F_L is the force in the actuator.

The shaking table array system is composed of multiple shaking tables. In addition to the force in the actuator and the interaction between the shaking table and specimen, the force acting on the shaking table also includes additional force generated by the nonsynchronous output of shaking tables. In this paper, the dual shaking tables with flexible connection specimen were analyzed as a numerical model. Figure 1 shows the mechanical model of the dual shaking tables with flexible connecting specimen.

The dynamic equilibrium equations of the tables and specimen can be written in terms of Laplace transform as

$$\left[M_p s^2 + 2(cs + k)\right] x_p - (cs + k) x_1 - (cs + k) x_2 = 0, \tag{4}$$

$$\left(M_T s^2 + cs + k\right) x_1 - (cs + k) x_p = F_1, \tag{5}$$

$$\left(M_T s^2 + cs + k\right) x_2 - (cs + k) x_p = F_2, \tag{6}$$

where M_p is the mass of the flexible connecting specimen, k is the connection stiffness coefficient between each table and specimen, c is the damping coefficient between each table and specimen, x_p is the relative displacement of the specimen, x_1 is the displacement of table 1, x_2 is the displacement of table 2, F_1 is the force in the actuator of the shaking table 1, and F_2 is the force in the actuator of the shaking table 2. Equations (4)–(6) can be simplified to

$$s^2 x_1 = \frac{F_1 + \left((cs+k)^2 / \left(M_p s^2 + 2(cs+k)\right)\right) x_2}{M_T + ((cs+k)/s^2) - \left((cs+k)^2 / \left(s^2 \left(M_p s^2 + 2cs + 2k\right)\right)\right)},$$

$$s^2 x_2 = \frac{F_2 + \left((cs+k)^2 / \left(M_p s^2 + 2(cs+k)\right)\right) x_1}{M_T + ((cs+k)/s^2) - \left((cs+k)^2 / \left(s^2 \left(M_p s^2 + 2cs + 2k\right)\right)\right)}. \tag{7}$$

Combining the dynamic equilibrium equations of the tables and specimen with the basic equations of the electrohydraulic servo-shaking table system, the basic equations

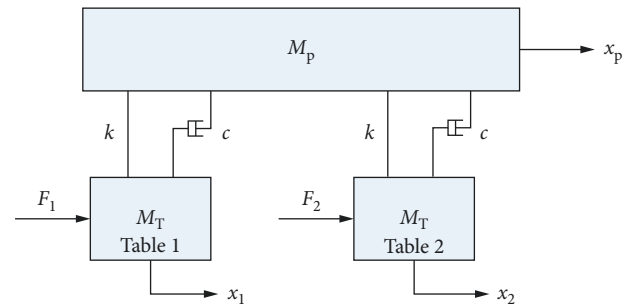

Figure 1: Mechanical model of dual shaking tables with specimen.

of the dual electrohydraulic servo-shaking table system with specimen can be written in terms of Laplace transform as

$$\begin{aligned}
&\left(M_p s^2 + 2cs + 2k\right) x_p - (cs + k) x_1 - (cs + k) x_2 = 0,\\
&\left[\left(M_T s^2 + cs + k\right) G_2 + s\right] x_1 - G_2 (cs + k) x_p = \frac{k_q}{A_p} x_{v1},\\
&\left[\left(M_T s^2 + cs + k\right) G_2 + s\right] x_2 - G_2 (cs + k) x_p = \frac{k_q}{A_p} x_{v2},
\end{aligned} \tag{8}$$

where

$$G_2 = \frac{V}{4\beta A_p^2} s + \frac{K_c + C_c}{A_p^2}. \tag{9}$$

In order to build the transfer function of dual shaking tables with specimen, three-variable feedback was introduced into the open-loop transfer function of the dual electrohydraulic servo-shaking tables, and second-order characteristics of the servo-valve and the sensor were considered. The transfer function block diagram of the system is shown in Figure 2.

The transfer function matrix of the dual shaking tables system with specimen is

$$\begin{Bmatrix} s^2 x_1 \\ s^2 x_2 \end{Bmatrix} = \begin{pmatrix} H_{11} & H_{12} \\ H_{21} & H_{22} \end{pmatrix} \begin{Bmatrix} u_{x1} \\ u_{x2} \end{Bmatrix}, \tag{10}$$

where

$$\begin{aligned}
H_{11} = H_{22} &= \frac{k_q G_{sv}}{A_p} G_3 \frac{\left(G_p G_{Ta} s^2 - G_2 G_{p1}^2\right)}{G_p G_{Ta}^2 s^2 - 2 G_2 G_{p1}^2 G_{Ta}},\\
H_{12} = H_{21} &= \frac{k_q G_{sv}}{A_p} G_3 \frac{G_2 G_{p1}^2}{G_p G_{Ta}^2 s^2 - 2 G_2 G_{p1}^2 G_{Ta}},\\
G_p &= M_p s^2 + 2cs + 2k,\\
G_{p1} &= cs + k,\\
G_{Ta} &= G_2 \frac{\left(M_T s^2 + cs + k\right)}{s^2} + \frac{1}{s} + \frac{k_q}{A_p} G_4,
\end{aligned} \tag{11}$$

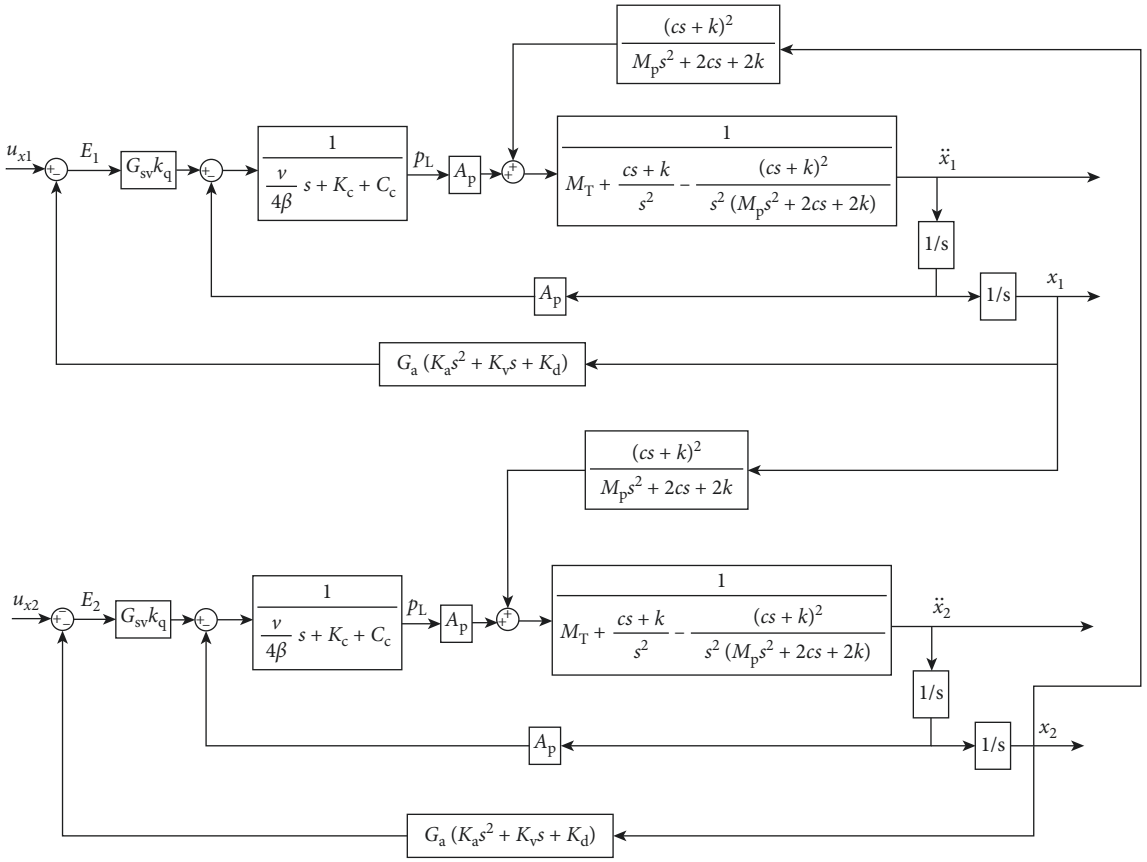

FIGURE 2: Transfer function block diagram of dual shaking tables with specimen.

where x_{v1} is the valve spool displacement of the shaking table 1, x_{v2} is the valve spool displacement of the shaking table 2, s^2x_1 is the acceleration of the shaking table 1, s^2x_2 is the acceleration of the shaking table 2, u_{x1} is the command signal of the shaking table 1, u_{x2} is the command signal of the shaking table 2, G_3 is the transfer function of the three-variable generator, G_4 is the transfer function of the three-variable feedback loop, G_{sv} is the transfer function of the electrohydraulic servo-valve when the flow gain is $k_q = 1$, H_{11} is the transfer function from the command signal of the shaking table 1 u_{x1} to the acceleration of the shaking table 1 s^2x_1, H_{12} is the transfer function from the command signal of the shaking table 1 u_{x1} to the acceleration of the shaking table 2 s^2x_2, H_{21} is the transfer function from the command signal of the shaking table 2 u_{x2} to the acceleration of the shaking table 1 s^2x_1, and H_{22} is the transfer function from the command signal of the shaking table 2 u_{x2} to the acceleration of the shaking table 2 s^2x_2.

The system performance effects on the dual shaking tables caused by the mass, frequency, and damping ratio of the flexible connecting specimen were obtained as shown in Figures 3–8. Figures 3, 5, and 7 show that the interaction effects on the transfer function H_{11} are characterized by a peak-notch distortion in the amplitude-frequency response at the natural frequency of the specimen and in a close frequency band. Figures 4, 6, and 8 show that the interaction effects on the transfer function H_{12} are characterized by a peak distortion in the amplitude-frequency response at the natural frequency of the specimen and in a close frequency band. Figures 3 and 4 present the effects of the specimen's mass on frequency response of transfer functions H_{11} and H_{12} when the frequency of the specimen is 5 Hz and the damping ratio of the specimen is 0.035. Comparison of the frequency response characteristic curves in Figure 3 indicates that the dual shaking tables-

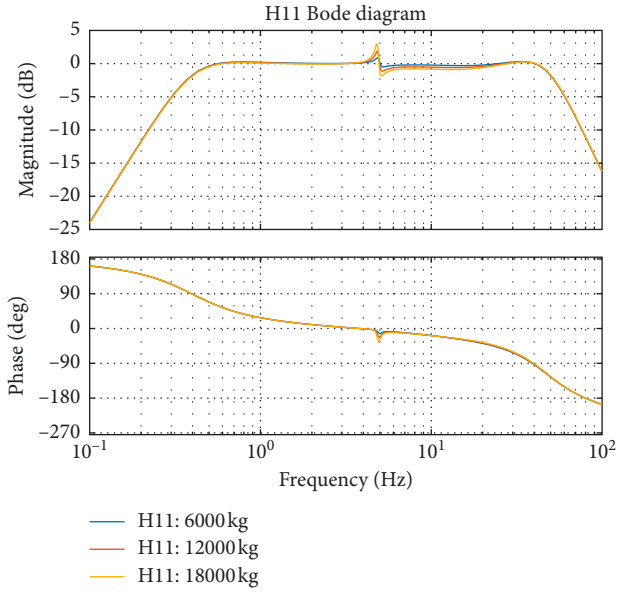

FIGURE 3: Effect of specimen's mass on frequency response of H_{11}.

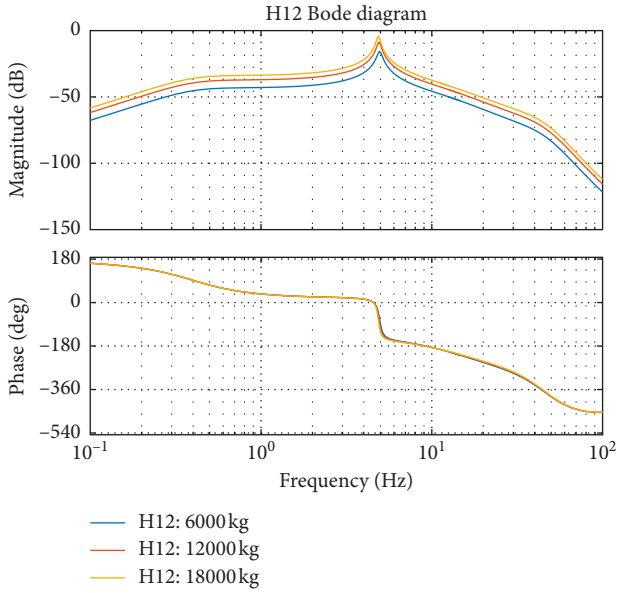

Figure 4: Effect of specimen's mass on frequency response of H_{12}.

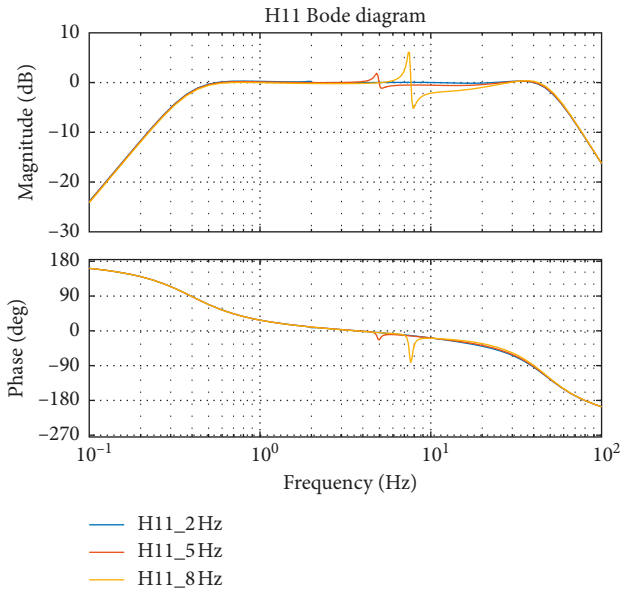

Figure 5: Effect of specimen's natural frequency on frequency response of H_{11}.

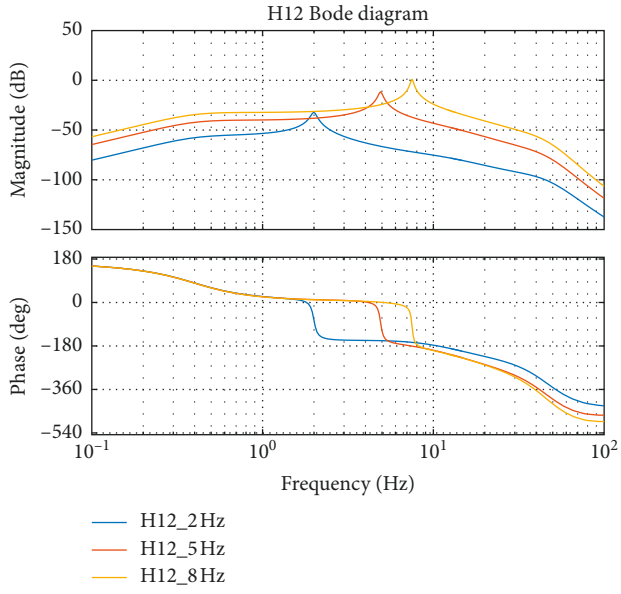

Figure 6: Effect of specimen's natural frequency on frequency response of H_{12}.

specimen interaction effect on transfer function H_{11} increases with the mass of the specimen. Comparison of the frequency response characteristic curves in Figure 4 indicates that the dual shaking tables-specimen interaction effect on the transfer function H_{12} also increases with the mass of the specimen. Figures 5 and 6 present the effect of specimen's frequency on frequency response of the transfer functions H_{11} and H_{12} when the mass of the specimen is 12000 kg and the damping ratio of the specimen is 0.035. Comparison of the frequency response characteristic curves in Figure 5 indicates that the dual shaking tables-specimen interaction effect on the transfer function H_{11} increases with the frequency of the specimen. Comparison of the frequency response characteristic curves in Figure 6 indicates that the dual shaking tables-specimen interaction effect on the transfer function H_{12} also increases with the frequency of the specimen. Figures 7 and 8 present the effects of the specimen's damping ratio on frequency response of transfer functions H_{11} and H_{12} when the mass of the specimen is 12000 kg and the frequency of the specimen is 5 Hz. Comparison of the Bode diagrams in Figure 7 indicates that the dual shaking tables-specimen interaction effect on the transfer function H_{11} decreases with the damping ratio of the specimen. Comparison of the Bode diagrams in Figure 8 indicates that the dual shaking tables-specimen interaction effect on the transfer function H_{12} also decreases with the damping ratio of the specimen. Comparing with the interaction effects generated by the single shaking table-specimen [7], the interaction effects generated by the dual shaking tables-specimen are more complicated and obvious.

3. Force Feedback Compensation for the Interaction Effects

Performance analysis of the dual shaking tables with specimen showed that the interaction effect on the transfer function H_{11} is characterized by a peak-notch distortion in the amplitude-frequency response at the natural frequency of the specimen and in a close frequency band, and the interaction effect on the transfer function H_{12} is characterized by a peak distortion in the amplitude-frequency response at the natural frequency of the specimen and in a close frequency band. The interaction generated by the specimen loaded on the dual shaking tables affected the output of the tables. In order to eliminate the interaction effects on system performance of the dual shaking tables, force feedback compensation was introduced into the existing three-variable control in this paper. The compensation principle is that the interaction can be calculated by

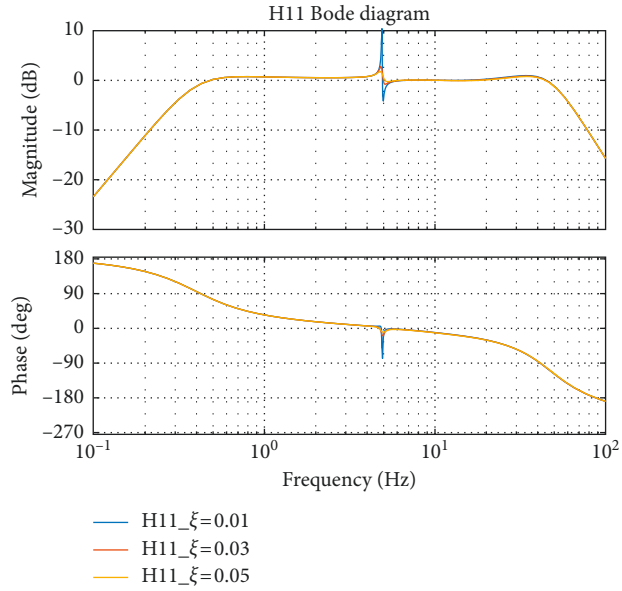

Figure 7: Effect of specimen's damping ratio on frequency response of H_{11}.

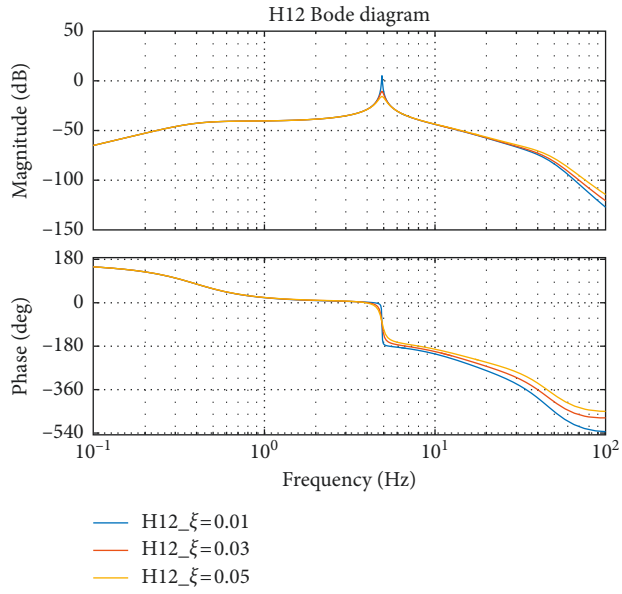

Figure 8: Effect of specimen's damping ratio on frequency response of H_{12}.

Equation (12), in which the force in the actuator F_L is measured by the force sensor, or the pressure difference between actuator chambers p_L is measured by the differential pressure sensor, and the acceleration of the table s^2x_T is measured by the acceleration sensor. Then, the compensation signal is formed by multiplying the interaction between the shaking table and specimen by the inverse transfer function from the valve spool displacement x_v to the force in the actuator F_L. The new equivalent drive signal is synthesized by the compensation signal negative feedback to the command signal. Figure 9 shows the block diagram of the dual shaking tables system in which force feedback compensation was applied to the block diagram in Figure 2.

The interaction between the dual shaking tables and specimen is

$$F_T = M_T s^2 x_T - F_L = M_T s^2 x_T - A_p p_L. \quad (12)$$

The inverse transfer function $G_{Fu}^{-1}(s)$ from the valve spool displacement x_v to the force in the actuator F_L obtained by Equations (1)–(3) is

$$G_{Fu}^{-1}(s) = \frac{x_v}{F_L} = \frac{M_T V s^2 + 4\beta M_T (K_c + C_c)s + 4\beta A_p^2}{4\beta A_p M_T G_{sv} k_q s}. \quad (13)$$

The compensation signal Δu can be expressed as

$$\Delta u = G_{Fu}^{-1}(s) F_T. \quad (14)$$

4. Simulation Analysis of the Control System of Dual Shaking Tables

In order to verify the control effect of the proposed method for the dual shaking tables loading with specimen, the dual electrohydraulic servo-shaking tables connected by the flexible specimen were selected for simulation. Table 1 shows the characteristic parameters of the dual electrohydraulic servo-shaking tables. The time history of El-Centro NS reduced 10 times scale was employed as the input signal. The simulation analysis of the dual electrohydraulic servo-shaking tables was conducted by using MATLAB/Simulink. Figure 10 shows the input signal.

A flexible specimen was selected for numerical simulation. The mass of the specimen is 12000 kg, the nature frequency of the specimen is 9 Hz, and the damping ratio of the specimen is 0.03. Figure 11 shows the Bode diagram of the transfer function H_{11} of the dual shaking tables system with specimen controlled by three-variable control and force feedback compensation. Comparison of three-variable control and force feedback compensation indicates that the Bode diagram of the transfer function H_{11} under three-variable control has a peak-notch distortion in the amplitude-frequency response at the natural frequency of the specimen and in a close frequency band. When force feedback compensation is introduced into three-variable control, the interaction effect on the transfer function H_{11} can be completely compensated. Figure 12 shows the Bode diagram of the transfer function H_{12} of the dual shaking tables system with specimen for the cases controlled by three-variable control and force feedback compensation. The Bode diagram of the transfer function H_{12} under three-variable control has a peak distortion in the amplitude-frequency response at the natural frequency of the specimen and in a close frequency band. As the acceleration of the shaking table 1 $s^2x_1 = H_{11}u_{x1} + H_{12}u_{x2}$, the acceleration of the shaking table 1 s^2x_1 is obviously influenced by the motion of the shaking table 2 in the natural frequency of the specimen and in a close frequency band. When force feedback compensation is introduced into three-variable control, the amplitude of the Bode diagram of the transfer function H_{12} is down from 7 dB to −40 dB at the natural frequency of the specimen. The interaction effect on the Bode diagram of the transfer function H_{12} is suppressed by

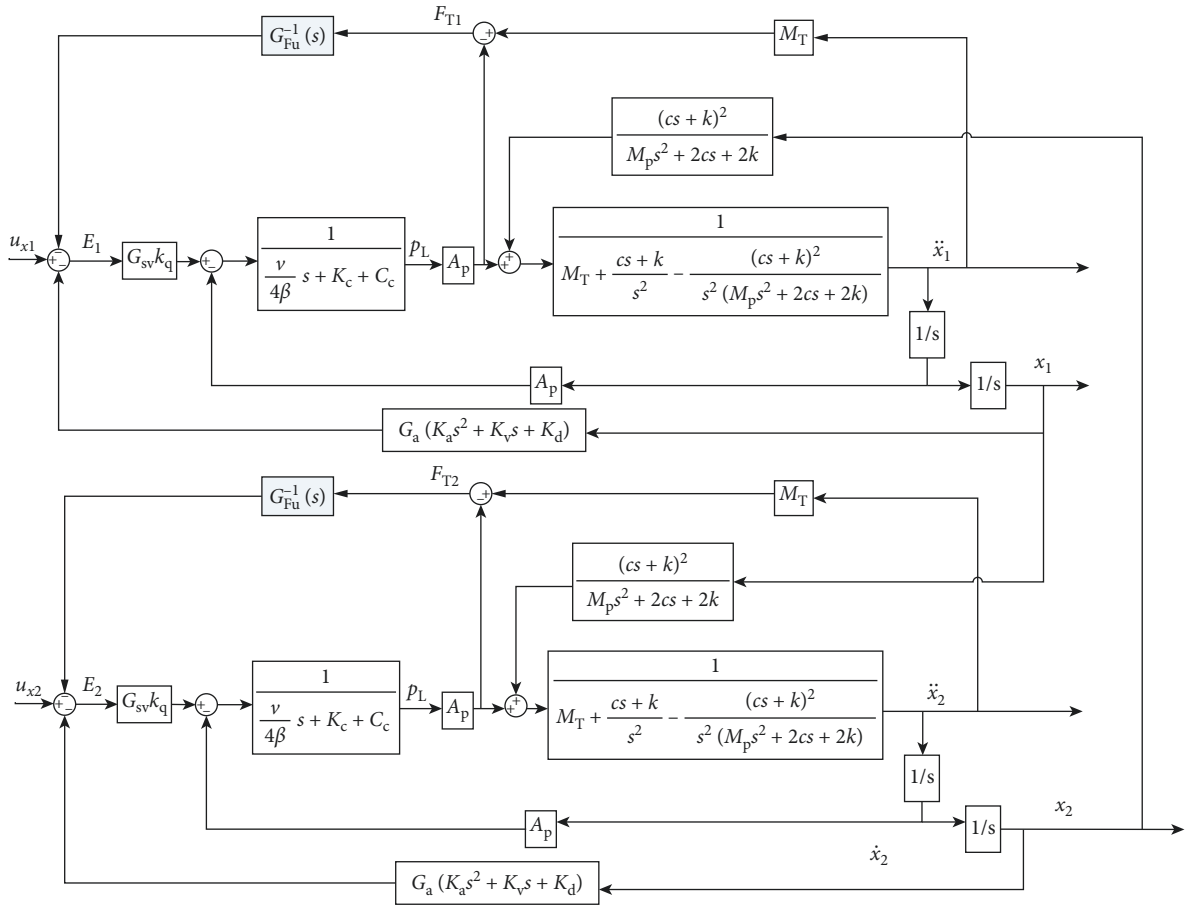

Figure 9: Block diagram of force feedback compensation of the dual shaking tables with specimen.

Table 1: Characteristic parameters of dual electrohydraulic servo-shaking tables.

Designation	Parameter
Table size	3 m × 3 m
Table mass	6000 kg
Maximum load	10000 kg
Frequency range	0.4 Hz~50 Hz
Natural frequency of sensor	150 Hz
Damping ratio of sensor	0.7
A_p	0.011 m^2
β	7×10^8 N/m^2
V	2.662×10^{-3} m^3
K_c	2.5×10^{-11} $m^5/(N\cdot s)$
Natural frequency of servo-valve	100 Hz
Damping ratio of servo-valve	0.7

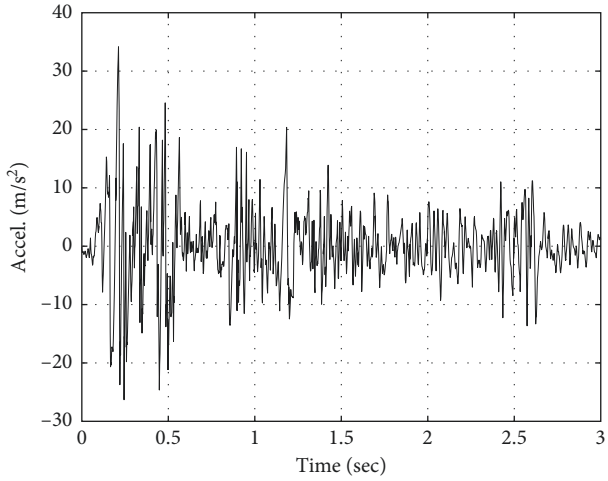

Figure 10: Earthquake motion input.

force feedback compensation. Figure 13 shows the acceleration time histories of the dual shaking tables without/with specimen under three-variable control. Figure 14 shows the acceleration time histories of the dual shaking tables with specimen under force feedback compensation and without specimen under three-variable control. Comparison of Figures 13 and 14 indicates that the acceleration time history of the dual shaking tables with specimen under force feedback compensation control coincides exactly with the acceleration time history of the dual shaking tables without specimen under three-variable control. Figure 15 shows the acceleration Fourier amplitude spectrum of the dual shaking tables without/with specimen under three-variable control. The interaction effect on the acceleration Fourier amplitude spectrum is manifested by a peak-notch distortion at the natural frequency of the specimen and in a close frequency band. Figure 16 shows the acceleration Fourier amplitude spectrum of the dual shaking tables with specimen under force feedback compensation and without specimen under

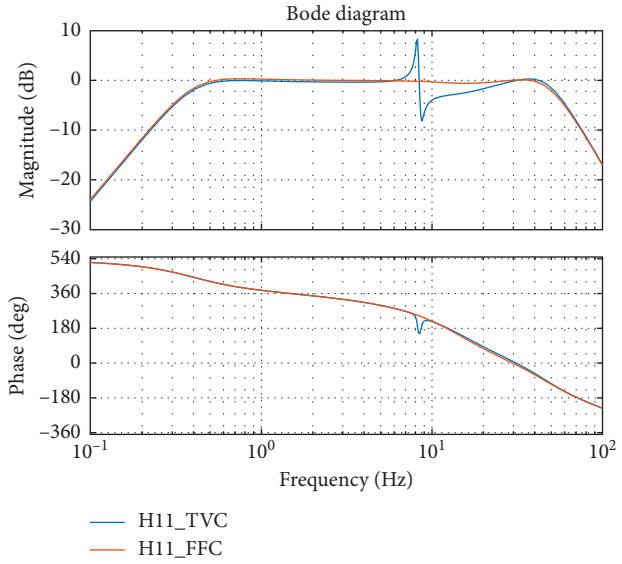

Figure 11: Bode diagram of transfer function H_{11}.

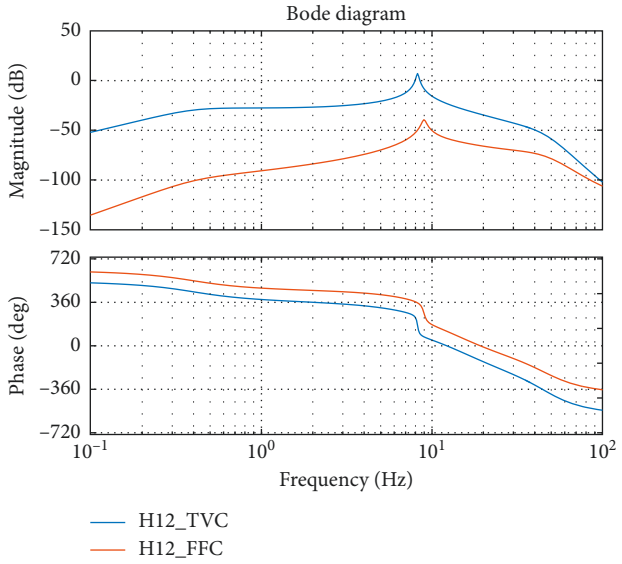

Figure 12: Bode diagram of transfer function H_{12}.

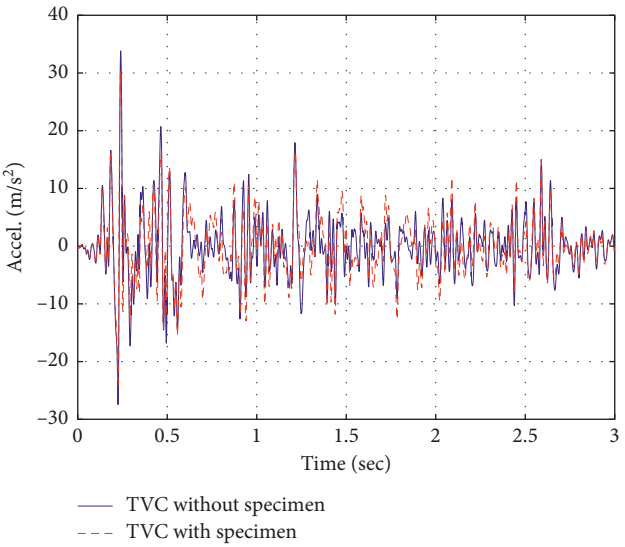

Figure 13: Acceleration time history of the dual shaking tables without/with specimen under TVC.

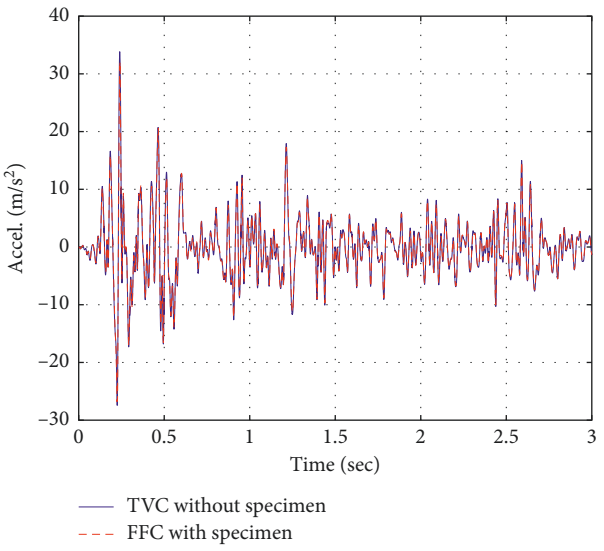

Figure 14: Acceleration time history of the dual shaking tables without/with specimen under TVC/FFC.

three-variable control. Comparison of Figures 15 and 16 indicates that the acceleration Fourier amplitude spectrum of the dual shaking tables with specimen under force feedback compensation control coincides exactly with the acceleration Fourier amplitude spectrum of the dual shaking tables without specimen under three-variable control. The peak-notch distortion in the acceleration Fourier amplitude spectrum caused by the specimen is well compensated by force feedback compensation introduced into three-variable control.

5. Simulation Analysis of Error Influence

Force feedback compensation proposed in this paper was based on the assumptions that the force in the actuator F_L and the acceleration of the table s^2x_T were measured accurately. Based on the above ideal state, the control effect of force feedback compensation for the interaction between the shaking table and specimen were analyzed. Actually, some errors in real time and accuracy of information acquisition and feedback might exist in the shaking table testing, such as the measurement of force in the actuator and the acceleration of the shaking table, and so on. Those errors have an effect on the control effect of force feedback compensation. The effects of force sensor error (or the differential pressure sensor error) and the acceleration sensor error on force feedback compensation were simulated for the interaction between the dual shaking tables and specimen.

Considering the errors of the force sensor or the differential pressure sensor and acceleration sensor, Equation

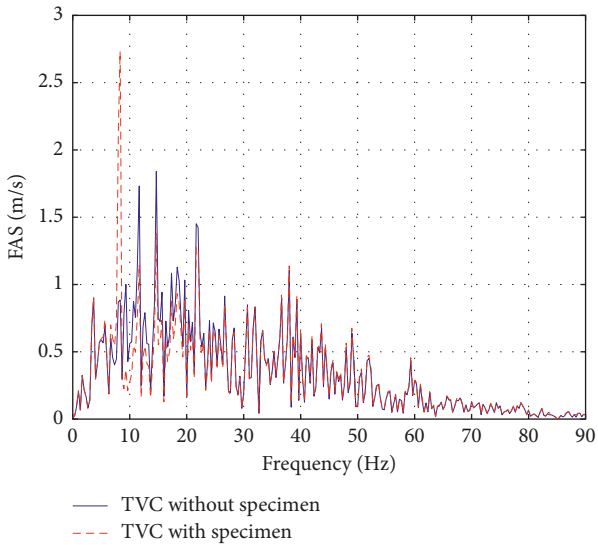

Figure 15: Acceleration Fourier amplitude spectrum of the dual shaking tables without/with specimen under TVC.

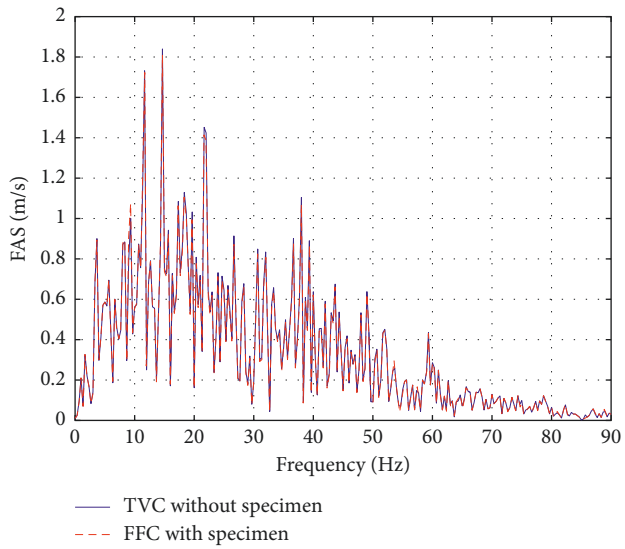

Figure 16: Acceleration Fourier amplitude spectrum of the dual shaking tables without/with specimen under TVC/FFC.

(12) of the interaction between the shaking table and specimen can be expressed as

$$F_T = (1-\alpha)M_T s^2 x_T - A_p(1-\gamma)p_L, \quad (15)$$

where α is the error coefficient of acceleration sensor and γ is the error coefficient of force sensor or differential pressure sensor.

Figures 17 and 18 present the effect of varying acceleration sensor error on the frequency characteristic of transfer functions H_{11} and H_{12} when the dual shaking tables with specimen are controlled by introducing force feedback compensation into three-variable control. The frequency characteristic curves, which are obtained by the error coefficient of the acceleration sensor varied from 0 percent to 15 percent, indicate that the effect caused by some error of

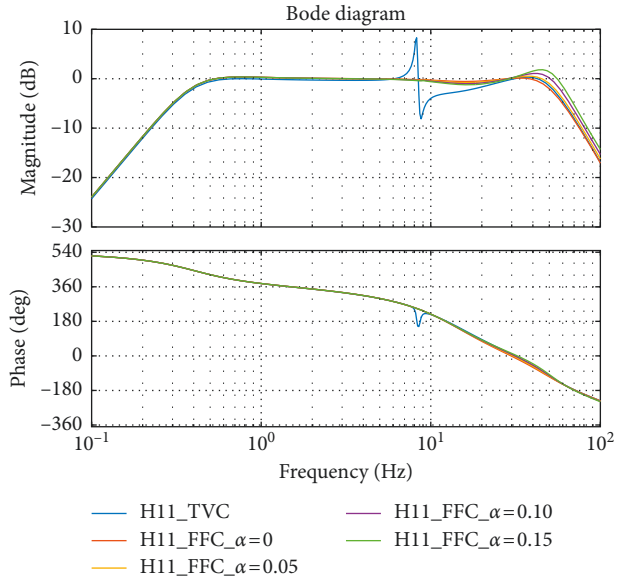

Figure 17: Effect of acceleration sensor error on the Bode diagram of H_{11}.

the acceleration sensor is characterized by a peak distortion in the high frequency of the amplitude-frequency response of the transfer functions H_{11} and H_{12}. However, the peak value in the amplitude-frequency response of the transfer function H_{11} caused by the acceleration sensor error is less than 3 dB, which is within the range of acceptable error. The peak in the amplitude-frequency response of the transfer function H_{12} caused by the acceleration sensor error is less than −50 dB. So the error effect caused by the acceleration sensor can be neglected. Therefore, the error of acceleration sensor does not significantly affect the interaction between the dual shaking tables and specimen compensated by introducing force feedback into three-variable control.

Figures 19 and 20 present the effect of varying force sensor error or differential pressure sensor error on the frequency characteristic of transfer functions H_{11} and H_{12} when the dual shaking tables with specimen are controlled by introducing force feedback into three-variable control. The frequency characteristic curves in Figure 19, which are obtained by the error coefficient of the force sensor or the differential pressure sensor varied from 0 percent to 15 percent, indicate that the effect caused by some error of force sensor or the differential pressure sensor is still characterized by a peak-notch distortion in the amplitude-frequency response of the transfer function H_{11} at the natural frequency of the specimen and in a close frequency band. However, the absolute values of the peak and notch are less than 3 dB. The effect of the force sensor error or the differential press sensor error on the compensation for the interaction effect can be neglected. At the same time, the high-frequency amplitude in the amplitude-frequency response of the transfer function H_{11} is slightly reduced by the error of the force sensor or the differential pressure sensor. A frequency band of 3 Hz can be reduced by per 5 percent error. Comparison of the frequency characteristic

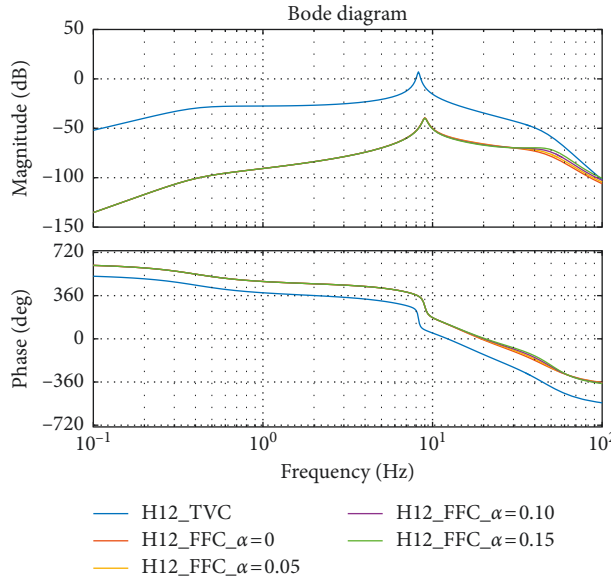

Figure 18: Effect of acceleration sensor error on the Bode diagram of H_{12}.

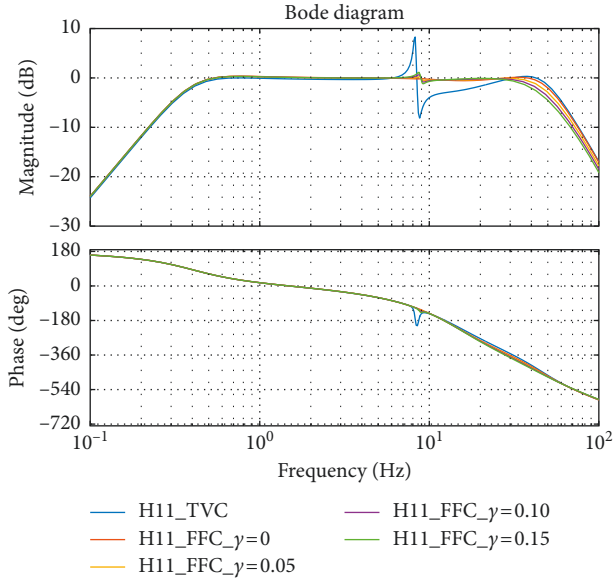

Figure 19: Effect of differential pressure sensor error on the Bode diagram of H_{11}.

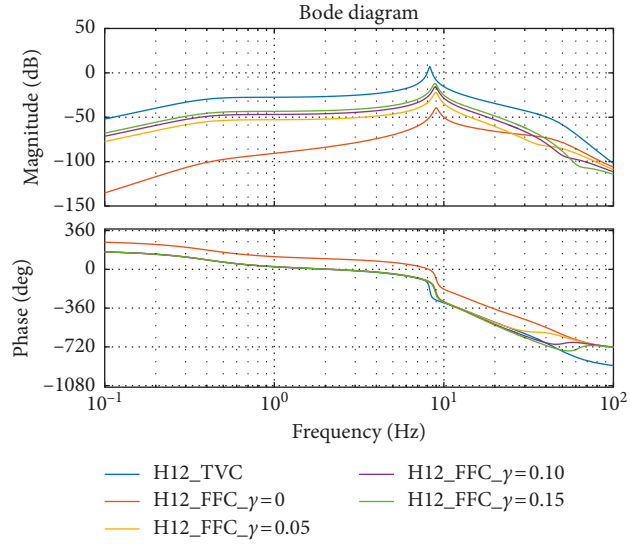

Figure 20: Effect of differential pressure sensor error on the Bode diagram of H_{12}.

curves in Figure 20 indicates that the peak distortion in the amplitude-frequency response of the transfer function H_{12} can be still suppressed by introducing force feedback into three-variable control. The amplitude of the peak distortion is down from 7 dB to −12 dB when the error of the force sensor or the differential pressure sensor is 15 percent. The control effect is slightly decreased by the error of the force sensor or the differential pressure sensor.

6. Conclusion

In the dual shaking tables test, the interaction force, which is generated by the specimen and nonsynchronous output of shaking tables, affects the system characteristics of the dual shaking tables; therefore, the precision of the output of the dual shaking tables is decreased. In order to improve the precision of the output of the dual shaking tables, the interaction effect and compensation on the system characteristics of the dual shaking tables with specimen were studied in this paper.

(1) The interaction effect on the transfer function from u_{x1} to s^2x_1 (H_{11}) was characterized by a peak-notch distortion in the amplitude-frequency response at the natural frequency of the specimen and in a close frequency band, and the interaction effect on the transfer function from u_{x1} to s^2x_2 (H_{12}) was characterized by a peak distortion in the amplitude-frequency response at the natural frequency of the specimen.

(2) In order to improve the output precision of the dual shaking tables, force feedback compensation was introduced into three-variable control to compensate the interaction between the dual shaking tables and specimen. The simulation analysis of the dual shaking tables with specimen shows that the interaction effect on the transfer function from u_{x1} to s^2x_1 (H_{11}) can be completely compensated, and the interaction effect on the Bode diagram of the transfer function from u_{x1} to s^2x_2 (H_{12}) can be suppressed by introducing force feedback compensation into three-variable control.

(3) The information acquisition and feedback errors of force in the actuator and the acceleration of the shaking table exist in the dual shaking tables testing. But the error influence on the system performance of the dual shaking tables was not obvious if the information acquisition and feedback errors were less than 15 percent. The error influence on the control effect of force feedback compensation can be neglected. Force feedback compensation can be applied to compensate the interaction between the dual shaking tables and specimen.

Data Availability

The data used to support the findings of this study are available from the corresponding author upon request.

Conflicts of Interest

The authors declare that there are no conflicts of interest regarding the publication of this paper.

Acknowledgments

This research was supported by the National Natural Science Foundation of China (Grant nos. 51738001, 51278013, 51508526, 51578024, and 51421005) and the opening foundation of Beijing Key Lab of Earthquake Engineering and Structural Retrofit.

References

[1] H. H. Huang, "Development of seismic simulation shaking table," *World Information on Earthquake Engineering*, vol. 1, pp. 47–51, 1985, in Chinese.

[2] C. Fang, "Status quo of earthquake simulating shaking table and its development," *World Information on Earthquake Engineering*, vol. 15, no. 2, pp. 89–91, 1999, in Chinese.

[3] Y. H. Wang, W. R. Cheng, F. Lu et al., "Development of the shaking table," *Earthquake Resistant Engineering and Retrofitting*, vol. 29, no. 5, pp. 53–56, 2007, in Chinese.

[4] H. H. Huang, *Design and Application of the Shaking Table*, Seismological Press, Beijing, China, 2008, in Chinese.

[5] Z. Y. Tang, Z. B. Li, J. B. Ji et al., "Development in shaking table control system," *Journal of Earthquake Engineering and Engineering Vibration*, vol. 29, no. 6, pp. 162–169, 2009, in Chinese.

[6] M. L. Yi, S. P. Cao, and Y. S. Liu, *Electro-Hydraulic Control Technology*, Huazhong University of Science and Technology Press, Wuhan, China, 2010, in Chinese.

[7] M. Blondet and C. Esparza, "Analysis of shaking table-structure interaction effects during seismic simulation tests," *Earthquake Engineering & Structural Dynamics*, vol. 16, no. 4, pp. 473–490, 1988.

[8] X. Li and S. Z. Tian, "Research on the reproductive accuracy of the earthquake wave in the earthquake simulating test," *Journal of Harbin Architecture and Civil Engineering Institute*, vol. 26, no. 4, pp. 110–115, 1993, in Chinese.

[9] S. J. Dyke, B. F. Spencer Jr., P. Quast, and M. K. Sain, "The role of control-structure interaction in protective system design," *Journal of Engineering Mechanics*, vol. 121, no. 2, pp. 322–338, 1995.

[10] A. L. Maoult, J. C. Queval, and R. Bairrao, "Dynamic interaction between the shaking table and the specimen during seismic tests," in *Advances in Performance-Based Earthquake Engineering. Geotechnical, Geological and Earthquake Engineering*, M. N. Fardis, Ed., vol. 13, pp. 431–440, Springer, Dordrecht, Netherlands, 2010.

[11] T. Trombetti, "*Analytical modeling of a shaking table system*," M.S. thesis, Rice University, Houston, TX, USA, 1996.

[12] J. P. Conte and T. L. Trombetti, "Linear dynamic modeling of a uni-axial servo-hydraulic shaking table system," *Earthquake Engineering & Structural Dynamics*, vol. 29, no. 9, pp. 1375–1404, 2000.

[13] T. L. Trombetti and J. P. Conte, "Shaking table dynamics: results from a test-analysis comparison study," *Journal of Earthquake Engineering*, vol. 6, no. 4, pp. 513–551, 2002.

[14] Z. B. Li, Z. Y. Tang, D. X. Zhou, J. B. Ji, and H. Ma, "The effects on the earthquake simulation caused by the characteristics of the specimen in the shaking table tests-part 1: the effects on the stability of the system," *Journal of Beijing University of Technology*, vol. 36, no. 8, pp. 1091–1098, 2010, in Chinese.

[15] Z. Y. Tang, Z. B. Li, D. X. Zhou, J. B. Ji, and H. Ma, "The effects on the earthquake simulation caused by the characteristics of the specimen in the shaking table tests-part 2: the effects on the replaying precision of the recorded seismic waves and the real-time compensation," *Journal of Beijing University of Technology*, vol. 36, no. 9, pp. 1199–1205, 2010, in Chinese.

[16] Y. Dozono, T. Horiuchi, H. Katsumata, and T. Konno, "Shaking-table control by real-time compensation of the reaction force caused by a nonlinear specimen," *Journal of Pressure Vessel Technology*, vol. 126, no. 1, pp. 122–127, 2004.

[17] M. Iwasaki, K. Ito, M. Kawafuku, H. Hirai, Y. Dozono, and K. Kurosaki, "Disturbance observer-based practical control of shaking tables with nonlinear specimen," in *Proceedings of the 16th IFAC World Congress (IFAC 2005)*, pp. 251–256, Elsevier, Prague, Czech, July 2005.

[18] K. Seki, M. Iwasaki, M. Kawafuku, and H. Hirai, "Improvement of control performance in shaking-tables by feedback compensation for reaction force," in *Proceedings of the 2008 34th Annual Conference of IEEE Industrial Electronics Conference (IECON2008)*, pp. 2551–2556, IEEE, Orlando, FL, USA, November 2008.

[19] K. Seki, M. Iwasaki, and H. Hirai, "Reaction force compensation with frequency identifier in shaking table systems," in *Proceedings of the 2010 11th IEEE International Workshop on Advanced Motion Control (AMC)*, pp. 673–678, IEEE, Nagaoka, Niigata, Japan, November 2010.

[20] B. M. Phillips, N. E. Wierschem, and B. F. Spencer Jr., "Model-based multi-metric control of uniaxial shake tables," *Earthquake Engineering & Structural Dynamics*, vol. 43, no. 5, pp. 681–699, 2014.

[21] P. Tian and Z. W. Chen, "Control strategy in earthquake simulation test based on elastic payload," *Journal of Vibration Engineering*, vol. 32, no. 5, pp. 26–32, 2013, in Chinese.

[22] X. J. Li, J. K. Wang, F. F. Li, N. Li, and H. H. Huang, "Differential movement synchronous tracking control strategy of double-shaking table system loading with specimen," *Shock and Vibration*, vol. 2018, Article ID 1785184, 11 pages, 2018.